Multimodal Measurements of Brain Tissue Metabolism and Perfusion in a Neonatal Model of Hypoxic-Ischaemic Injury

Gemma Bale, Ajay Rajaram, Matthew Kewin,
Laura Morrison, Alan Bainbridge, Linshan Liu,
Udunna Anazodo, Mamadou Diop,
Keith St Lawrence, and Ilias Tachtsidis

Abstract

This is the first multimodal study of cerebral tissue metabolism and perfusion post-hypoxic-ischaemic (HI) brain injury using broadband near-infrared spectroscopy (bNIRS), diffuse correlation spectroscopy (DCS), positron emission tomography (PET) and magnetic resonance spectroscopy (MRS). In seven piglet preclinical models of neonatal HI, we measured cerebral tissue saturation (StO_2), cerebral blood flow (CBF), cerebral oxygen metabolism ($CMRO_2$), changes in the mitochondrial oxidation state of cytochrome c oxidase (oxCCO), cerebral glucose metabolism (CMRglc) and tissue biochemistry (Lac+Thr/tNAA). At baseline, the parameters measured in the piglets that experience HI (not controls) were $64 \pm 6\%$ StO_2, 35 ± 11 ml/100 g/min CBF and 2.0 ± 0.4 µmol/100 g/min CMRO2. After HI, the parameters measured were $68 \pm 6\%$ StO_2, 35 ± 6 ml/100 g/min CBF, 1.3 ± 0.1 µmol/100 g/min $CMRO_2$, 0.4 ± 0.2 Lac+Thr/tNAA and 9.5 ± 2.0 CMRglc. This study demonstrates the capacity of a multimodal set-up to interrogate the pathophysiology of HIE using a combination of optical methods, MRS, and PET.

Keywords

Near-infrared spectroscopy · Diffuse correlation spectroscopy · Metabolism · Hypoxic ischaemic encephalopathy

G. Bale (✉) · I. Tachtsidis
Biomedical Optics Research Laboratory, University College London, London, UK
e-mail: g.bale@ucl.ac.u

A. Rajaram · M. Kewin · L. Morrison · L. Liu · U. Anazodo · M. Diop · K. S. Lawrence
Medical Biophysics, Western University, and Lawson Health Research Institute, London, ON, Canada

A. Bainbridge
Medical Physics, University College London Hospital, London, UK

32.1 Introduction

Hypoxic-ischaemic encephalopathy (HIE) is responsible for a quarter of neonatal deaths globally and is one of the largest causes of preventable childhood disabilities such as cerebral palsy [1]. The injury evolves throughout treatment, so a continuous monitoring of brain tissue health deployed at the cotside is highly desirable. The progression of the brain health during HIE can be

characterised in terms of the metabolism, progressing from a 'latent phase' where metabolism recovers, to normal levels, to 'secondary energy failure' which may cause further injury. The metabolic state after HIE can be measured using proton (^{1}H) magnetic resonance spectroscopy (MRS) [2]. The ^{1}H MRS-derived thalamic Lac/NAA peak area ratio is a robust predictor of neurodevelopmental outcome in babies with HIE and has been used as a surrogate outcome measure in clinical neuroprotection studies of HIE. This metabolic information is vital for prognostication but only gives a snapshot of the cerebral injury at a particular time point, usually after treatment has been completed. Glucose consumption, measured by FDG PET, is valuable but is also non-continuous and requires injection of radioisotopes so is not ideal for neonatal care [3].

Diffuse optics provides a continuous measurement of brain metabolism. Broadband near-infrared spectroscopy (bNIRS) yields information about cerebral haemodynamics (via oxy- and deoxyhaemoglobin: HbO$_2$ and HHb, respectively), tissue oxygenation (StO$_2$) and metabolism from cytochrome c oxidase (CCO). CCO is the terminal electron acceptor in the electron transport chain (ETC): the final stage of oxidative metabolism [4]. We have recently shown that the signal is associated with the level of HI injury [5]. Another optical technique, diffuse correlation spectroscopy (DCS), measures an index of cerebral blood flow, which, combined with oxygenation from NIRS and pulse oximetry, measures cerebral metabolic rate of oxygen (CMRO$_2$) [6]. We have recently shown that it is possible to simultaneously measure CBF and CCO [7]; the aim of this study is to demonstrate how through a combination of optics (bNIRS, DCS), FDG PET and MR measurements we can obtain a full description of the haemodynamic, oxygenation and metabolism status of the brain following HI.

32.2 Methods

32.2.1 Animal Model of HI

This study was approved by the Animal Use Subcommittee of the Canadian Council on Animal Care at Western University (London, Ontario). Piglets were anesthetised under 3% isoflurane during preparatory surgery (2% post surgery), tracheotomised and mechanically ventilated on an oxygen-medical air mixture. Incisions were made lateral to the trachea, and vascular occluders were placed around the carotid arteries posterior to the clavicle (In Vivo Metric, CA). Catheters were inserted into an ear vein for injections and into a femoral artery to monitor vitals (SurgiVet, Smiths Medical, MN), as well as to collect arterial blood samples for gas and glucose analyses. SaO$_2$ was measured via a pulse oximeter attached to the piglet's right forelimb. The bNIRS and DCS emission/detection fibres were secured to the piglet's left brain, avoiding the sagittal sinus, using an in-house 3D-printed probe holder.

The HI insult was induced by first inflating the occluders around the carotid arteries, followed by reducing the inspired oxygen from 21% to 8%. bNIRS and DCS data were acquired continuously throughout the insult, starting 5 minutes prior to carotid clamping to acquire baseline measurements. The real-time DCS flow index was used to confirm successful clamping, i.e. an immediate drop in CBF. Following this confirmation, inspired oxygen concentration was reduced, and the HI insult was maintained for a minimum duration of 10 minutes once the blood flow index reached its nadir. At the end of the HI insult, recovery was initiated by deflating the carotid occluders and returning oxygen supply to baseline levels.

Data were recorded from seven newborn piglets (four female, aged 10–40 hours): severe HI injury was induced in five piglets and there were two controls.

32.2.2 Measurements of Cerebral Metabolism

Cerebral metabolism was assessed by different modalities: bNIRS and DCS continuously before, during and after the HI and MRS and PET after HI.

The optical device has been fully described previously [7] and is described here briefly. Essentially, it is a bNIRS device and a DCS

device which were run synchronously with a system of shutters to avoid crosstalk between them. The bNIRS device consists of a halogen bulb (Ocean Optics HL-2000-HP) and a custom-made spectrometer (iDus Andor camera, Oxford Instruments; P&P Optica, ON, Canada). For the DCS system, the light source was a long coherence length, continuous-wave laser emitting at 785 nm (DL785–100 s, CrystaLaser, NV) and the detector a single-photon counting module (SPCM-AQR4C, Excelitas, QC, Canada). The output of the SPCM was fed into a correlator board (Flex033LQ-1, Correlator.com, NJ) to generate normalised intensity autocorrelation functions.

The continuous recording of bNIRS and DCS data was set on a 14 s cycle, acquiring 12 bNIRS spectra over 3 s, followed by two DCS measurements over the following 10s, with a 0.5 s delay. These measurements were collected continuously before, during and after HI. Ninety min post HI, the DCS data was calibrated by measuring absolute CBF by DCE-NIRS [8]. The DCE-NIRS protocol consisted of a bolus injection of indocyanine green (ICG, 0.1 mg/kg) into a cannulated vein. The CBF was measured by monitoring the cerebral ICG concentration with bNIRS and the time-varying arterial ICG concentration by a dye densitometer attached to a front paw (DDG 2001, Nihon Kohden, Japan).

Magnetic resonance imaging and spectroscopy and FDG PET were performed after the optical monitoring on a 3 T Biograph mMR scanner (Siemens Healthcare). MR scans included measurements of (lactate + threonine)/(NAA + NAAG) (Lac+Thr/tNAA) from the left hemisphere cortex (ant) and thalamus (bas) with proton (^{1}H) MRS (PRESS: TR = 2 s; TE = 135 or 288 ms) (Fig. 32.1).

32.2.3 Data Analysis

bNIRS: The changes in chromophore concentrations (oxCCO, HbO$_2$ and HHb) were calculated from the measured changes in broadband near-infrared light attenuation using the modified Beer-Lambert law as applied with the UCLn algorithm [4] across 136 wavelengths (771–906 nm) with a fixed differential path length factor of 4.39 (preterm head) and 3 cm optode separation. To measure absolute StO$_2$, the spectral data were analysed using the solution to the diffusion approximation for a semi-infinite medium [9]. The absorption coefficient was defined as the sum of the three largest chromophores: HHb, HbO$_2$ and water. Chromophore concentrations and the scattering terms were determined in a series of steps involving fitting the numerical derivatives of the theoretical model (i.e. the analytical solution to the diffusion approximation) to the derivative spectra.

An algorithm was developed to quantify the recovery of Δ[HbT], Δ[HbDiff], Δ[oxCCO], StO$_2$ and CBF 1 hour after HI. Data at baseline and recovery were averaged over a 1 min window to calculate the recovery fraction of each signal relative to baseline. All the measurements were normalised against the nadir point:

$$\text{Recovery Fraction} \left(\text{RF} \right) = \frac{\text{Recovery} - \text{Nadir}}{\text{Baseline} - \text{Nadir}} \times 100\%$$

MRS data were analysed using Tarquin [10]. The fitted amplitudes of Lac and Thr were combined because they are not resolvable in in vivo spectra [11].

32.3 Results

Measured attenuation spectra and autocorrelation curves from this data set have been previously presented [7]. Figure 32.2 presents an example of the optical signals obtained and the resulting recovery fractions. The full results with all final absolute metabolic variables are shown in Table 32.1. At baseline, the parameters measured in the piglets that experienced HI (not controls) were 64 ± 6% StO$_2$, 35 ± 11 ml/100 g/min CBF and 2.0 ± 0.4 μmol/100 g/min CMRO$_2$. After HI, the parameters measured were 68 ± 6% StO$_2$, 35 ± 6 ml/100 g/min CBF, 1.3 ± 0.1 μmol/100 g/min CMRO$_2$, 0.4 ± 0.2 Lac+Thr/tNAA and 9.5 ± 2.0 CMRglc.
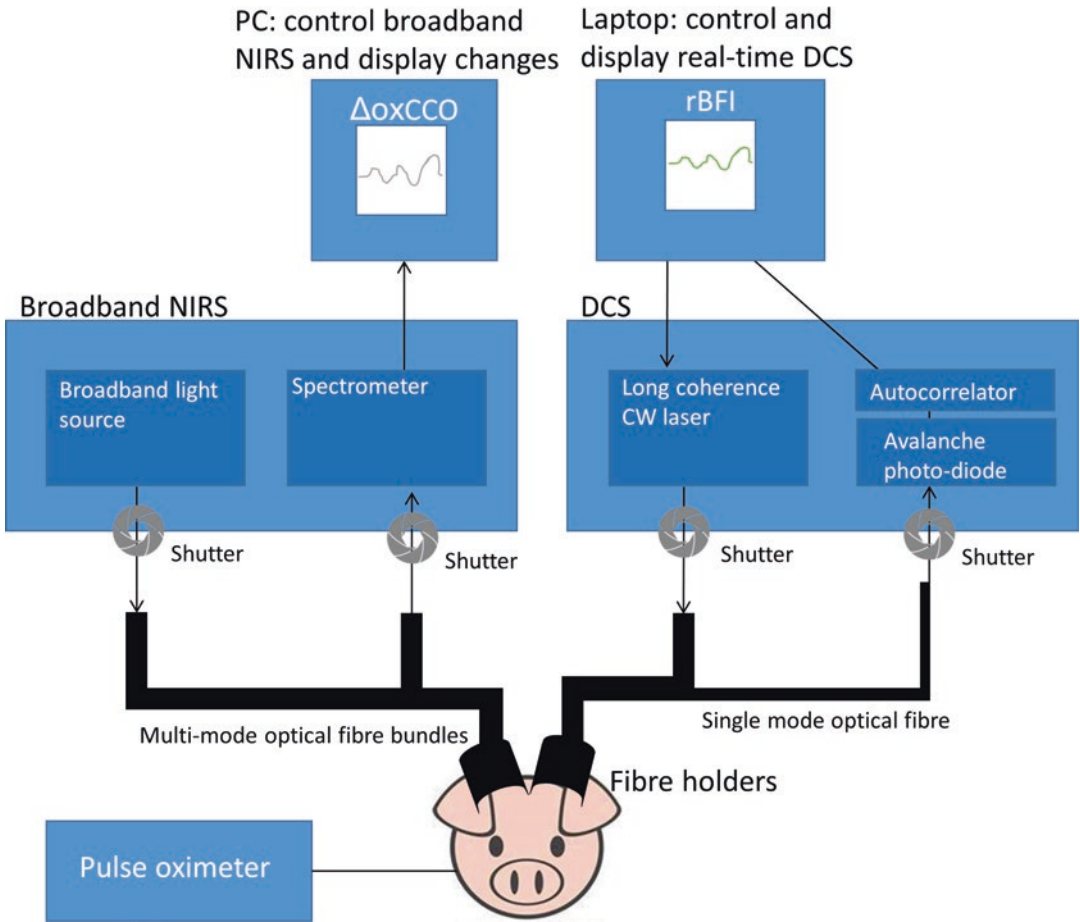
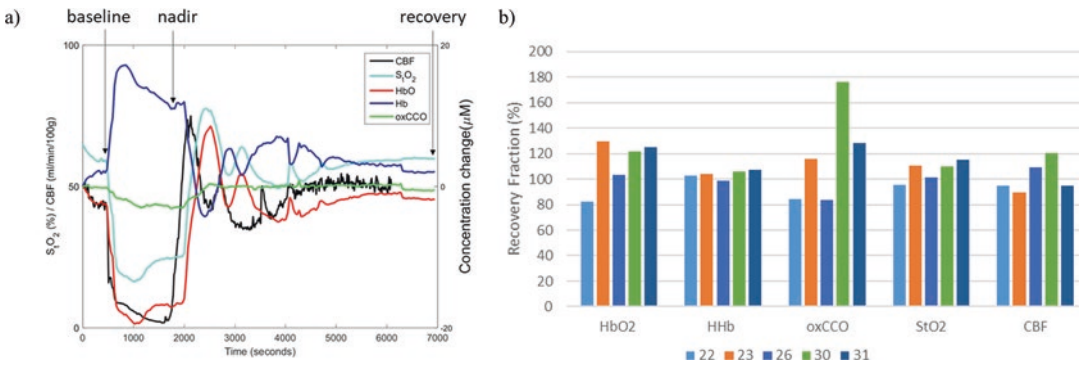**Fig. 32.1** Optical instrumentation for continuous broadband NIRS and DCS measurements

Fig. 32.2 (**a**) Example of optical signals used to calculate recovery fraction (from piglet 26). (**b**) Recovery fractions 1 hour after HI for all optical signals for all HI piglets

Table 32.1 Piglet details and final cerebral measurements. Units: CBF ml/100 g/min, CMRO$_2$ μmol/100 g/min, MRS is Lac+Thr/total NAA and CMRglc μmol/100 g/min. MRS data is missing in some anatomical locations for some animals due to low SNR

Pig	Age (hours)	Weight (kg)	Sex	HI (mins)	StO$_2$ (%)	CBF	CMRO$_2$	MRS Ant	MRS Bas	CMRglc
20	12	1.4	F	0	65.2	33.6	1.2		0.04	8.44
22	23	1.2	F	10	70.4	35.7	1.2		0.11	8.58
23	10	1.6	M	20	71.7	39.2	1.4		0.57	7.04
26	24	1.5	M	20	64.1	42.0	1.2	0.24	0.35	13.20
28	28	1.9	F	0	45.2	45.5	3.9	0.20	0.29	13.72
30	20	1.8	M	20	75.4	30.8	1.4	0.37	0.39	9.58
31	40	1.7	F	20	59.0	26.6	1.3	0.45		9.10

32.4   Discussion

In this work, we have demonstrated the ability of optical monitoring (bNIRS and DCS) to obtain metabolic information aligned with ^{1}H MRS and FDG PET in a piglet model of HIE. Further, due to the non-invasive, cotside nature of the optical devices, we highlight the potential for continuous measurements of metabolism. The measured parameters are aligned with those obtained by another device working alone; Kaynezhad et al. observed similar changes in HbO$_2$, HHb and oxCCO during a piglet model of HI [12], and the BFI changes are comparable to those obtained by Rajaram et al. [7].

The recovery fractions obtained with bNIRS and DCS showed that all signals recovered to around 100%, showing that the brain was able to recover to normal levels of oxygenation and metabolism after the insult suggesting that the injury was mild [13]. These optical measures agree with the results from the MR-PET which shown little difference in the recovered metabolic parameters between the control animals and the animals who experienced HI. This may be due to the measurements (both optical and MR-PET) being obtained within the first few hours post HI when the piglets are likely to be in the 'latent phase' of HIE.

This is one of the limitations of this study. Other limitations include the low number of animals involved due to technical issues with the multimodal monitoring which restricts our ability to perform statistical analysis at this stage. Future work includes increasing the number of animals

studied and increasing the time between insult and final measurement to capture the metabolic decline during secondary energy failure.

References

1. Chalak LF, Tian F, Tarumi T, Zhang R (2016) Cerebral hemodynamics in asphyxiated newborns undergoing hypothermia therapy: pilot findings using a multiple-time-scale analysis. Pediatr Neurol 55:30–36
2. Mitra S et al (2019) Proton magnetic resonance spectroscopy lactate/N-acetylaspartate within 2 weeks of birth accurately predicts 2-year motor, cognitive and language outcomes in neonatal encephalopathy after therapeutic hypothermia. Arch Dis Child Fetal Neonatal Ed 104(4):F424–F432
3. Thorngren-Jerneck K et al (2001) Cerebral glucose metabolism measured by positron emission tomography in term newborn infants with hypoxic ischemic encephalopathy. Pediatr Res 49(4):495–501
4. Bale G, Elwell CE, Tachtsidis I (2016) From Jöbsis to the present day: a review of clinical near-infrared spectroscopy measurements of cerebral cytochrome-c-oxidase. J Biomed Opt 21(9):091307
5. Bale G et al (2019) Oxygen dependency of mitochondrial metabolism indicates outcome of newborn brain injury. J Cereb Blood Flow Metab 39(10):2035–2047
6. Durduran T, Choe R, Baker WB, Yodh AG (2010) Diffuse optics for tissue monitoring and tomography. Reports Prog Phys 73(7):076701
7. Rajaram A et al (2018) Simultaneous monitoring of cerebral perfusion and cytochrome c oxidase by combining broadband near-infrared spectroscopy and diffuse correlation spectroscopy. Biomed Opt Express 9(6):2588–2603

8. Cooper JA et al (2011) Continuous monitoring of absolute cerebral blood flow by near-infrared spectroscopy during global and focal temporary vessel occlusion. J Appl Physiol 110(6):1691–1698

9. Yeganeh HZ, Toronov V, Elliott JT, Diop M, Lee T-Y, Lawrence KS (2012) Broadband continuous-wave technique to measure baseline values and changes in the tissue chromophore concentrations. Biomed Opt Express 3(11):2761–2770

10. Wilson M, Reynolds G, Kauppinen RA, Arvanitis TN, Peet AC (2011) A constrained least-squares approach to the automated quantitation of in vivo (1)H mag-netic resonance spectroscopy data. Magn Reson Med 65(1):1–12

11. Kreis R, Hofmann L, Kuhlmann B, Boesch C, Bossi E, Hüppi PS (2002) Brain metabolite composition during early human brain development as measured by quantitative in vivo 1H magnetic resonance spectroscopy. Magn Reson Med 48(6):949–958

12. Kaynezhad P et al (2019) Quantification of the severity of hypoxic-ischemic brain injury in a neonatal preclinical model using measurements of cytochrome-c-oxidase from a miniature broadband-near-infrared spectroscopy system. Neurophotonics 6(04):1